PNAS
www.pnas.org

Supplementary Information for

Storage of carbon reserves in spruce trees is prioritized over growth in the face of carbon limitation

Jianbei Huang*, Almuth Hammerbacher*, Jonathan Gershenzon, Nicole M. van Dam, Anna Sala, Nate G. McDowell, Somak Chowdhury, Gerd Gleixner, Susan Trumbore and Henrik Hartmann

*Jianbei Huang; *Almuth Hammerbacher
Email: hjianbei@bgc-jena.mpg.de; almuth.hammerbacher@fabi.up.ac.za

This PDF file includes:

Supplementary text (method and results)
Figures S1 to S5

Other supplementary materials for this manuscript include the following:

Dataset S1 Averaged aboveground daytime carbon assimilation and nighttime respiration, averaged fresh biomass increment, and the isotopic signature of the aboveground nighttime respiration and biomass.

Dataset S2 Concentrations of glucose, sucrose, fructose, starch, lipids and amino acids, and the isotopic signature of water soluble carbon and bulk

Dataset S3 Comparison of the full transcriptional responses between the control (positive carbon balance) versus the low carbon availability treatments (neutral and negative carbon balance)

Supplementary Information Text

Method

The C flux during hour *i* was assumed to be constant within the 2 h cycle and calculated using equation:

$$C_i\ (\mathrm{mg\ h^{-1}}) = ([CO_2]_{in} - [CO_2]_{out})(\mu\mathrm{mol\ mol^{-1}}) \times \frac{\mathrm{VFR\ (l\ min^{-1})} \times 60\ \mathrm{min} \times 12\ (\mathrm{g\ mol^{-1}})}{22.4\ (\mathrm{l\ mol^{-1}}) \times 1000}$$

where $[CO_2]_{in}$ and $[CO_2]_{out}$ are the $[CO_2]$ of air entering and exiting the chambers, respectively; VFR is volumetric flow rate of air passing through the chamber (c. 22 l min^{-1}); the molar volume of gas is 22.4 l mol^{-1} under normal conditions.

All $\delta^{13}C$ values were reported relative to the international Vienna Pee Dee Belemnite (VPDB), and calculated using equation:

$$\delta^{13}C(‰) = \left[\frac{\left[\frac{^{13}C}{^{12}C}\right]_{sample}}{\left[\frac{^{13}C}{^{12}C}\right]_{VPDB}} - 1 \right] \times 1000$$

To calculate $\delta^{13}C$ of aboveground biomass and substrate, $\delta^{13}C$ of bulk and water soluble carbon was weighted across young needles (yn), old needles (on), young branches (yb) and old branches (ob), using equation:

$$\mathrm{Weighted}\ \delta^{13}C = w_{yn} \times \delta^{13}C_{yn} + w_{on} \times \delta^{13}C_{on} + w_{yb} \times \delta^{13}C_{yb} + w_{ob} \times \delta^{13}C_{ob}$$

where w represents relative weight (%) of total carbon or water soluble carbon content of a corresponding tissue.

Results on the expression levels of genes

Overall responses. We identified genes encoding enzymes of pathways involving 26 pathways. More genes were significantly affected under negative carbon balance (i.e. carbon starvation, CS) than under neutral carbon balance (carbon compensation point, CCP), averaging 12% and 39%, respectively. Changes in the expression level of these genes were overall more pronounced under CS than CCP. In addition, we found that the homologous genes often showed opposite responses to declining carbon availability.

Photosynthesis. We identified 52, 46 and 91 contigs encoding enzymes involved in photosynthesis light reaction, photosynthesis dark reaction and light-harvesting pigments,

respectively. Overall, there was no significant difference in the expression level of most genes between control and CCP. However, under CS, the percentage of genes that were significantly downregulated was 75%, 50% and 24% for photosynthesis light reaction, photosynthesis dark reaction and light-harvesting pigments, respectively.

Specifically, under CS, there was a significant decrease in the expression levels of genes encoding chlorophyll a-b binding proteins, photosystem I and II reaction center subunits, the major steps in the Calvin–Benson–Bassham cycle, a glyceraldehyde-3-phosphate dehydrogenase and a triose phosphate transporter, as well as the elements of the cytochrome B6-f complex and chlorophyll biosynthesis. By contrast, we found an increase for the genes encoding a photosystem II CP47 protein (a chlorophyll binding protein in the core structure of PSII, a thylakoid luminal protein (psbP domain-protein), β-carotene biosynthesis, and two chlorophyllases that catalyzes the hydrolysis of ester bond in chlorophyll to yield chlorophyllide and phytol) ($p < 0.01$). Interestingly, both CCP and CS significantly increased the expression of genes encoding ribulose bisphosphate carboxylase (RuBisCO), the small chain of RuBisCO and the transketolase enzyme ($p < 0.01$).

Respiration. We identified 51, 32, 25 and 145 contigs for glycolysis/gluconeogenesis process, TCA cycle, pentose phosphate pathway and oxidative electron transport chain, respectively. We found no significant change in the expression level for more than 90% of the genes under CCP. However, a further reduction to CS caused proportionally more genes to be up- or down-regulated. For example, in the glycolysis pathway, approximately 34% of genes were significantly repressed while 14% increased under CS; the opposite trends were observed for TCA cycle and pentose phosphate pathway, where more genes were up-regulated (28% and 32%, respectively) rather than down-regulated (18% and 16%, respectively). The oxidative electron transport chain was not strongly affected under CS, with only 8 % of the genes involved increased and 14 % decreased.

For glycolysis/gluconeogenesis and TCA cycle, the expression of homologous genes often showed opposite trends. For example, a homologue of an ATP-dependent 6-phosphofructokinase 2, catalyzing the first committed step in glycolysis, was up-regulated in both treatments ($p < 0.01$), while the expression of a different homologue of this gene was down-regulated under CS. Under CS, a hexokinase 1 homologue was also significantly up-regulated, while hexokinase 3 was down-regulated ($p < 0.01$). An ATP-citrate synthase homologue involved in TCA cycle was down-regulated under both treatment conditions ($p < 0.05$), but the expression of another homologue of this gene was significantly higher in the CS ($p < 0.01$). In addition, the expression of 3 homologues of malate dehydrogenase was down-regulated under CS, while two were up-regulated and the expression of four contigs with the same homology showed no statistically significant change in expression. The CS treatment also resulted in an increased expression of

other enzymes involved in the TCA cycle, including isocitrate dehydrogenase, citrate synthase, succinate dehydrogenase and succinate CoA-ligase ($p<0.05$).

For the pentose phosphate pathway, the expression level of genes encoding glucose-6-phosphate 1-dehydrogenase and transaldolase expression were significantly up-regulated in both CPP and CS ($p < 0.01$) while a ribose-5-phosphate isomerase and a 6-phosphogluconolactonase gene were significantly down-regulated under CS.

For the oxidative electron transport chain, the expression of a NADH dehydrogenase [ubiquinone] iron-sulfur protein and a mitochondrial cytochrome B gene significantly increased under CCP and CS, while the expression of a cytochrome B5-like gene and a cytochrome B-C1 complex subunit gene significantly decreased, relative to control. The expression of several other genes, including genes encoding NADH dehydrogenase subunits, cytochrome C oxidase subunits, cytochrome B-C1 complex subunits as well as various proteins involved in the assembly of the cytochrome C complex were significantly down-regulated under CS ($p < 0.05$).

Starch and disaccharide. We identified 15 and 29 contigs encoding enzymes of starch and disaccharide (e.g. sucrose) biosynthesis, respectively. The expression levels of these genes were overall higher under CCP and CS compared to the control. Reducing carbon availability to CCP significantly increased 27% and 10% of the genes associated with starch and disaccharide biosynthesis, respectively ($p < 0.05$), while none of the genes were significantly repressed. Under CS, more genes were upregulated (40% and 31%) rather than downregulated for starch and disaccharide biosynthesis, respectively. The upregulated genes are mostly associated with starch and sucrose synthase enzymes.

For starch degradation, we identified 34 contigs, of which approximately 26% were significantly affected by CCP. More genes were significantly affected under CS, where 34% of the genes were up-regulated ($p < 0.05$). Both CCP and CS increased the expression of genes encoding β- and α-amylases, which degrade starch by exo- and endo-hydrolysis, respectively. By contrast, genes associated with β-glucosidases, which hydrolyze terminal sugars to release glucose, were significantly repressed under both CCP and CS.

Cellulose, pectin and hemicellulose biosynthesis. We identified 50 and 42 contigs that are putatively involved in the biosynthesis of cellulose and pectin/hemicellulose, respectively. Under CCP, genes associated with cellulose biosynthesis were either upregualted (16%) or downregulated (20%), while most genes (>83%) involved in pectin/hemicellulose biosynthesis were not significantly affected. Under CS, approximately 45% of the genes associated with cellulose biosynthesis to be downregulated, and 31% and 17% of the genes involved in pectin/hemicellulose biosynthesis were upregulated and downregulated, respectively($p < 0.05$).

Reducing carbon availability significantly decreased the transcript levels of genes involved in the cellulose synthase-like proteins (E1, E6 and G3) and xyloglucan biosynthesis ($p < 0.01$). Expression of genes encoding cellulose synthase A catalytic subunits, the enzyme responsible for beta-1,4-glucan microfibril crystallization and cell wall formation, was mostly similar to control. By contrast, both CCP and CS significantly increased the expression of genes encoding cellulose synthase interactive proteins, cellulose synthase-like protein H1, and a pectin biosynthesis gene encoding UDP-glucuronate 4-epimerase 1. Under CS, there was a significant increase in genes encoding xyloglucan glycosyltransferase for biosynthesis of hemicellulose ($p < 0.01$).

We also identified 51 genes encoding enzymes involved in cell wall lossening, an important process of cell expansion. Under CCP, most of the genes (>85%) were not significantly affected. Under CS, 28% and 18% of the genes are significantly repressed, in average by six times, and 18% of the genes were induced, in average by two times.

Cell wall degradation. We identified 194 contigs putatively involved in cell wall degradation. More than 80% of the genes were not significantly affected under CCP. However, under CS, there was a significant increase in the expression level of 33% of the genes, particularly those involved in beta-glucosidase responsible for cellulose degradation and as well as β-xylosidases, β-galactosidases and α-arabinofuranosidases involved in hemicellulose degradation. Only 17% of the genes were repressed ($p < 0.05$), including those encoding the xyloglucan endotransglucosylase/hydrolase proteins, as well as the polygalacturonases and the pectin esterases involved in pectin degradation.

Lipid biosynthesis. We identified 112, 84, 53 and 23 contigs encoding enzymes that catalyze the synthesis of fatty acid, sterol, triacylglycerol and phospholipid, respectively. Under CCP, we did not observe significant changes in the expression of most genes (>90%), except that 15 % of the genes associated with sterol biosynthesis were down-regulated. Under CS, however, approximately 30% of genes were significantly downregulated in all the pathways related to lipid biosynthesis.

For fatty acid biosyntheisis of, the transcription of genes encoding long-chain acyl-CoA synthetases and 3-ketoacyl-CoA synthases was consistently up-regulated in both CCP and CS compared to the control ($p < 0.05$) while the expression of acyl carrier proteins and the enzymes responsible for their synthesis were reduced ($p < 0.05$).

For sterol biosynthesis, 3-Oxo-delta(4,5)-steroid 5-beta-reductase involved in vascular strand development was significantly up-regulated under low carbon availability. By contrast, the expression of two enzymes in the mevalonate pathway which provides the precursors for sterol biosynthesis was significantly down-regulated in both low carbon availability treatments ($p <$

0.01). These included 3-hydroxy-3-methylglutaryl-coenzyme A reductase, catalyzing the rate-limiting step of the pathway and acetyl-CoA acetyltransferase.

For triacylglycerol synthesis, at CCP only one contig was up-regulated (phospholipid:diacylglycerol acyltransferase) and one contig down-regulated (diacylglycerol O-acyltransferase) with statistical support ($p < 0.05$). Under CS, homologs of phosphatidate phosphatase were upregulated while the transcript abundance of glycerol-3-phosphate acyltransferases and diacylglycerol O-acyltransferases were significantly reduced ($p < 0.05$).

For phospholipid biosynthesis, A fatty acid desaturase homologue was significantly up-regulated in both CCP and CS, while the transcription of a number of other homologues of this gene was significantly down-regulated.

Lipid degradation. For lipid degradation, we identified 61, 27 and 132 contigs involved in fatty acid degradation, triacylglycerol degradation and diverse lipases, respectively. The expression levels of most genes (> 85%) did not significantly change after reducing carbon availability to CCP. However, under CS, approximately 43% of the genes involved in fatty acid degradation were significantly upregulated; genes associated with triacylglycerol degradation and lipases were either upregulated (26% and 18%, respectively) or downregulated (26% and 14%, respectively).

The transcription of long-chain-alcohol oxidases was significantly up-regulated under low carbon availability. In particular, the glyoxylate cycle was strongly upregulated under both CCP and CS, with 42% and 62% of the genes being significantly increased relative to control ($p < 0.05$), respectively, including contigs encoding enzymes involved in every step of the pathway. The transcript abundance of triacylglycerol lipase and phospholipase A – D family proteins were also up-regulated under both CCP and CS, while the expression of genes encoding GDSL esterase/lipase and phospholipase A1 family proteins, diacylglycerol lipases and monoacylglycerol lipases were generally reduced ($p < 0.01$).

Protein and amino acid biosynthesis. We identified 648 and 143 contigs putatively involved in the biosynthesis of proteins and amino acids, respectively. The expression levels of most genes (>80%) were not significantly affected under CCP, while CS caused more genes associated with protein and amino acid degradation to be upregulated (13% and 22%, respectively) or downregulated (17% and 20%, respectively).

Reducing carbon availability increased the transcript abundances of specific contigs encoding amino acid-tRNA ligases as well as eukaryotic translation initiation factor and elongation factor proteins ($p < 0.05$). By contrast, the transcript abundances of contigs encoding different ribosomal subunits were reduced ($p < 0.05$). For amino acids, the expression of genes in the shikimate

pathway, involved in the synthesis of phenylalanine, tyrosine and tryptophan, were significantly increased under reduced carbon availability. These include homologues of shikimate kinase, phospho-2-dehydro-3-deoxyheptonate aldolase, phenylalanine hydroxylase, arogenate dehydratase/prephenate dehydratase and arogenate dehydrogenase. However, other homologues of phospho-2-dehydro-3-deoxyheptonate aldolase and arogenate dehydratase/prephenate dehydratase were significantly repressed. Furthermore, contigs encoding delta-1-pyrroline-5-carboxylate synthase involved in proline synthesis, dihydroxy-acid dehydratase involved in isoleucine biosynthesis, 2-isopropylmalate synthase involved in leucine synthesis and glutamate synthase were all upregulated under low carbon availability.

Protein and amino acid degradation. We identified 667 and 180 contigs encoding enzymes involved in protein and amino acid degradation, respectively. Under CCP, there was no significant change in the expression level for more than 85% of the genes. However, a further reduction to CS significantly increased 19% and 28% of the genes associated with protein and amino acid degradation, respectively, while 15% of the genes were significantly repressed in both pathways.

We found contrasting responses of the genes encoding different protein proteases. There was a significant up-regulation of genes for aspartic proteases involved in drought avoidance through abscisic acid signaling, inactive ATP-dependent zinc metalloproteases involved in chloroplast development, E3 ubiquitin-protein ligases, CO_2-response secreted proteases (controlling stomatal development) and for ATP-dependent zinc metalloproteases. By contrast, transcription was down-regulated for aspartyl protease family proteins, mitochondrial inner membrane proteases, Do-like proteases and subtilisin-like proteases ($p < 0.05$).

Reducing carbon availability induced the expression of genes involved in many pathways, including: asparagine synthetase involved in hydrolyzing glutamine, the transcriptional activity of arginase, ornithine aminotransferase and ornithine carbamoyltransferase involved in the arginine degradation pathway/ proline biosynthesis pathway; homologues of branched chain amino transferase, 2-oxoisovalerate dehydrogenase and 3-ketoacyl-CoA thiolase involved in the degradation of branched-chain amino acids; alanine and glutamate glyoxylate amino transferases and malate synthase involved in photorespiration; tyrosine aminotransferase, 4-hydroxyphenylpyruvate dioxygenase, fumarylacetoacetase and homogentisate 1,2-dioxygenase involved in phenylalanine and tyrosine degradation; and methionine gamma-lyase homologs. By contrast, homologues of tryptophan aminotransferase, cysteine desulfurase, acetyl-CoA acetyltransferase (ornithine cycle/mevalonate pathway), fumarylacetoacetase (degradation of aromatic amino acids) and glutamate/aspartate-prephenate aminotransferase were transcriptionally down-regulated ($p < 0.05$).

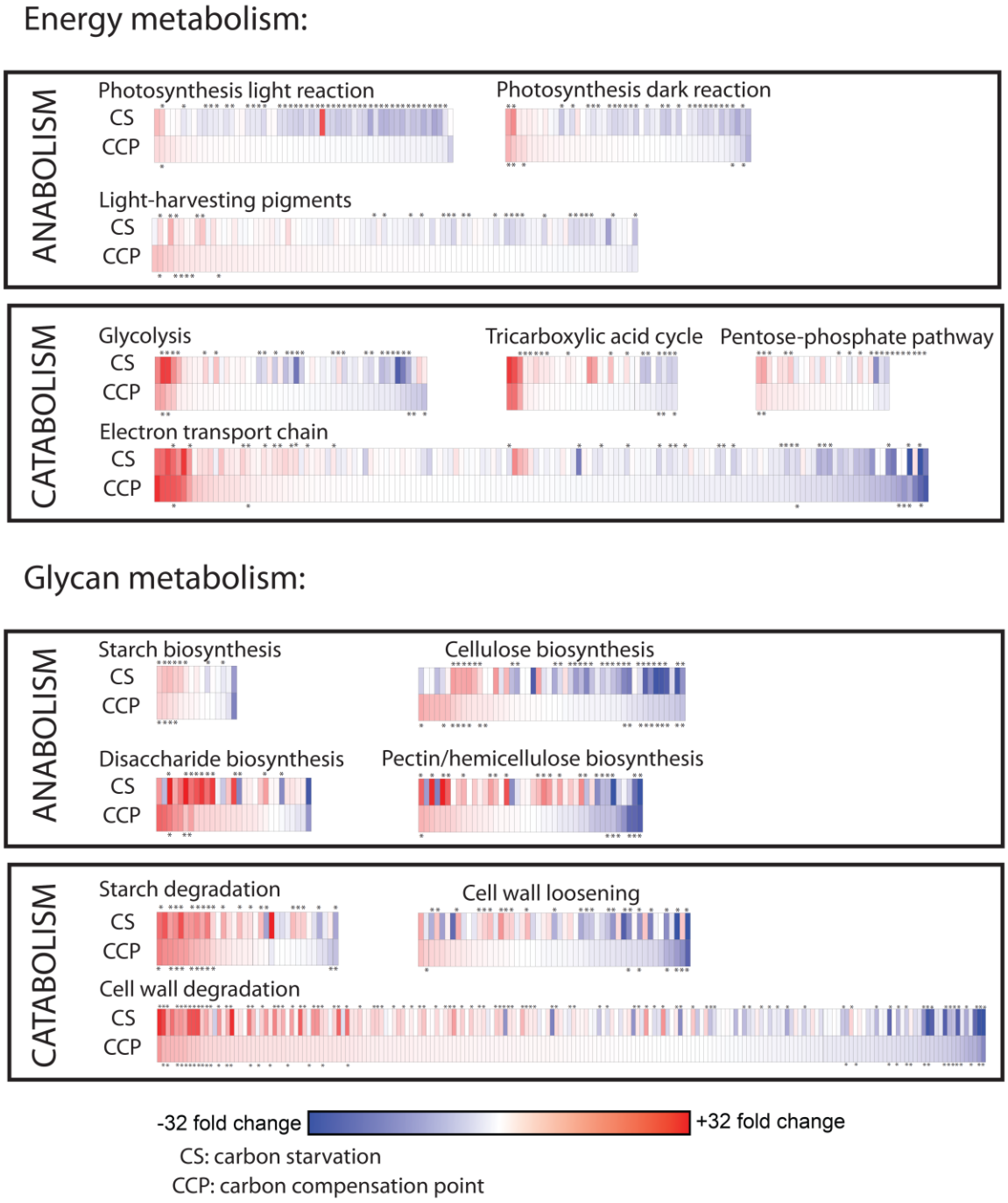

Fig. S1. Transcriptional regulation of energy and glycan metabolism. The gene expression patterns for young developing leaves under neutral (i.e., carbon compensation point, CCP) and negative carbon balance (carbon starvation, CS) at week 4. Each bar is composed of a number of genes (small boxes) with different expression patterns, starting from the repressed genes (blue) on the left side to the induced ones (red) on the right side. Asterisks indicate statistically significant differences ($P < 0.05$).

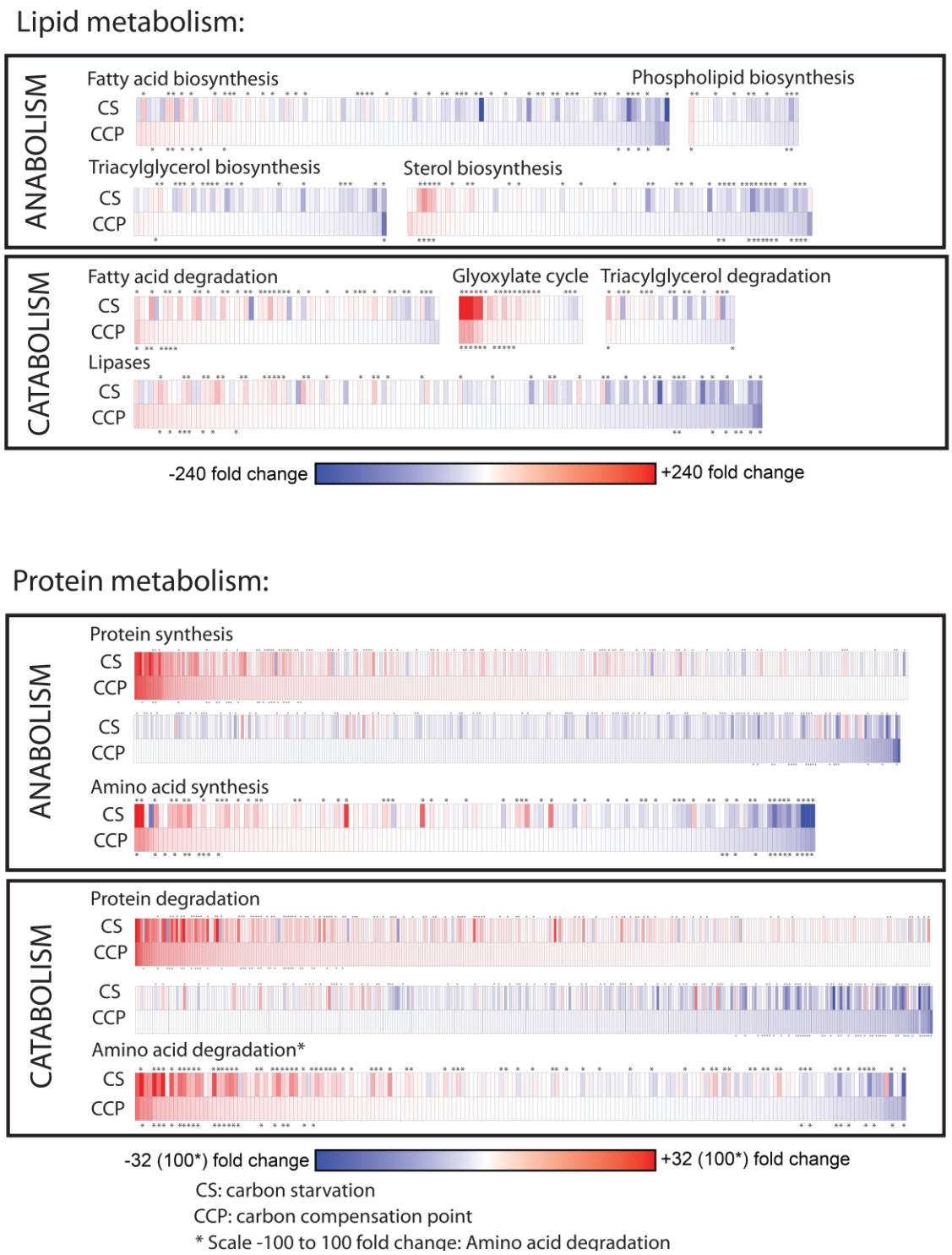

Fig. S2. Transcriptional regulation of lipid and protein metabolism. The gene expression patterns for young developing leaves under neutral (i.e., carbon compensation point, CCP) and negative carbon balance (carbon starvation, CS) at week 4. Each bar is composed of a number of genes (small boxes) with different expression patterns, starting from the repressed genes (blue) on the left side to the induced ones (red) on the right side. Asterisks indicate statistically significant differences ($P < 0.05$).

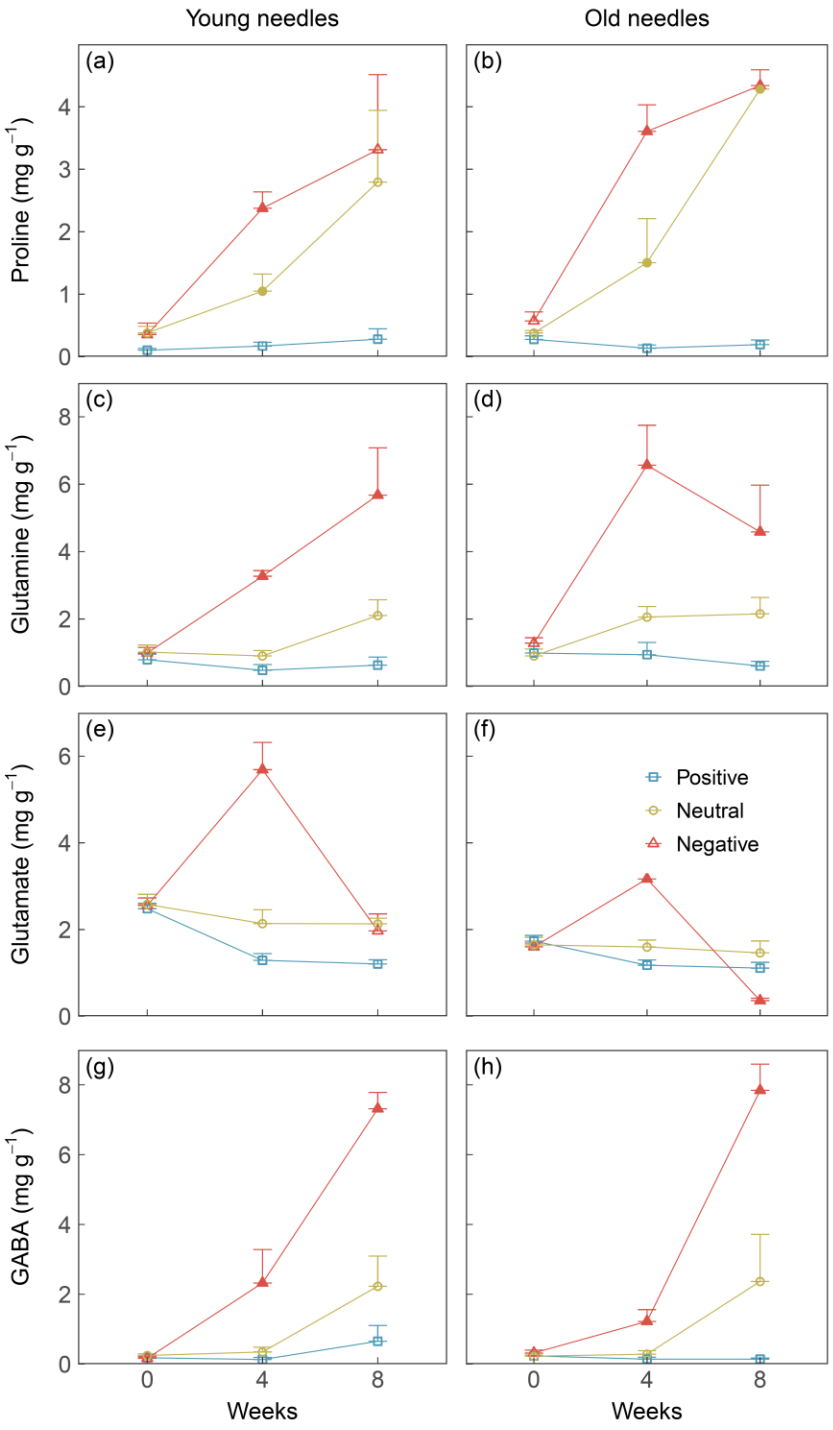

Fig. S3. Temporal dynamics of proline, glutamine, glutamate, and gamma-aminobutyric acid (GABA) in current year young and previous year old needles under declining carbon (C) balance. All data are expressed as concentrations (mg/g). Values are the means of four individual chambers (n=4); error bars represent SE. Significant differences between the low C availability treatments (neutral and negative C balance) and control (positive C balance) are calculated and indicated by filling of symbols ($P<0.05$).

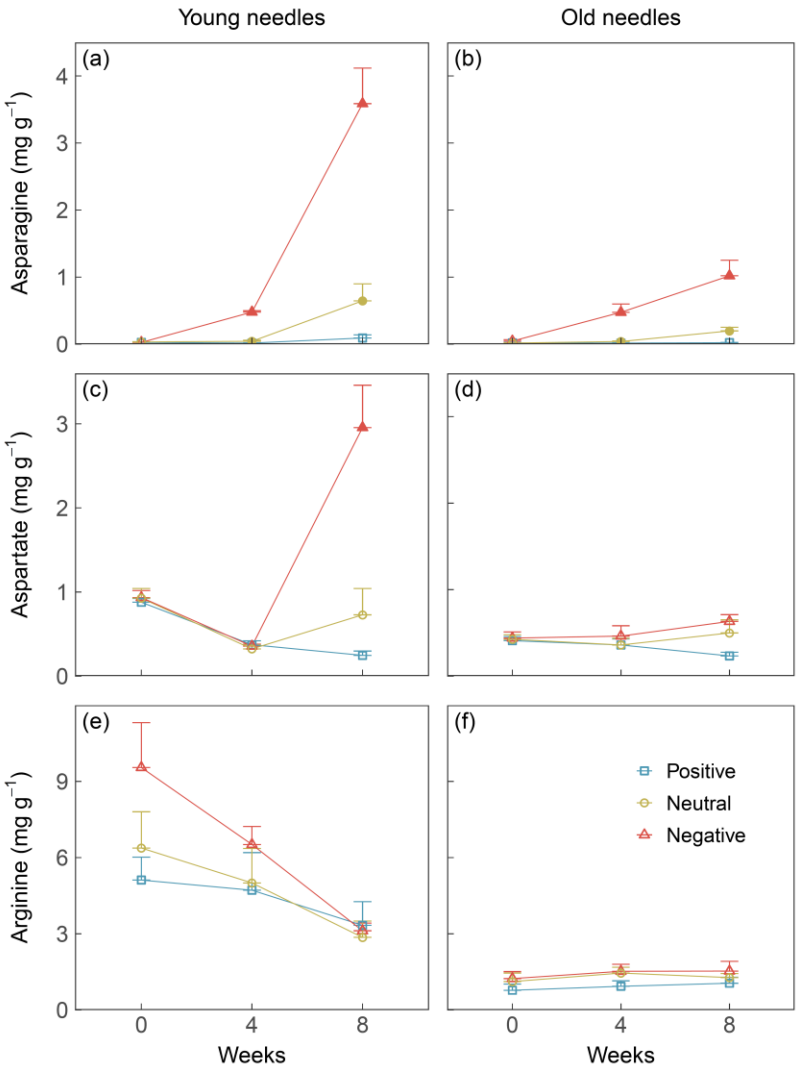

Fig. S4. Temporal dynamics of asparagine, aspartate, and arginine in current year young and previous year old needles under declining carbon (C) balance. All data are expressed as concentrations (mg/g). Values are the means of four individual chambers (n=4); error bars represent SE. Significant differences between the low C availability treatments (neutral and negative C balance) and control (positive C balance) are calculated and indicated by filling of symbols ($P<0.05$).

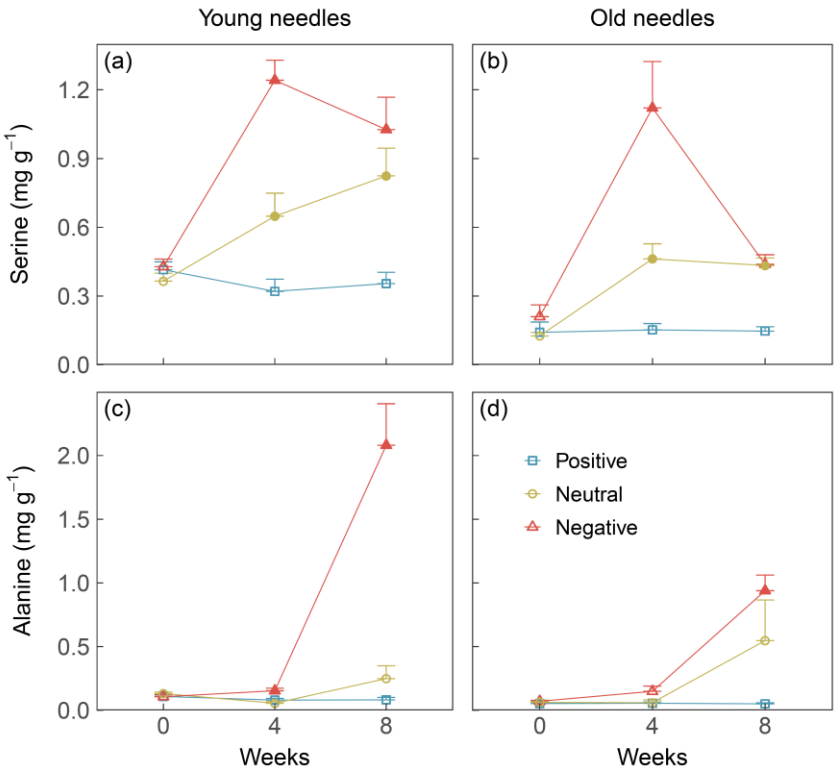

Fig. S5. Temporal dynamics of serine and alanine in current year young and previous year old needles under declining carbon (C) balance. All data are expressed as concentrations (mg/g). Values are the means of four individual chambers (n=4); error bars represent SE. Significant differences between the low C availability treatments (neutral and negative C balance) and control (positive C balance) are calculated and indicated by filling of symbols ($P<0.05$).

Dataset S1 Averaged aboveground daytime carbon assimilation and nighttime respiration, averaged fresh biomass increment, and the isotopic signature of the aboveground nighttime respiration and biomass.

Dataset S2 Concentrations of glucose, sucrose, fructose, starch, lipids and amino acids, and the isotopic signature of water soluble carbon and bulk

Dataset S3 Comparison of the full transcriptional responses between the control (positive carbon balance) versus the low carbon availability treatments (neutral and negative carbon balance)